

Mechanism of the decomposition of adsorbed methanol over a Pd/ α,β -Ga₂O₃ catalyst

Sebastián E. Collins, Miguel A. Baltanás, Adrian L. Bonivardi*

Instituto de Desarrollo Tecnológico para la Industria Química (INTEC), Güemes 3450, S3000GLN Santa Fe, Argentina

Received 22 April 2005; received in revised form 28 July 2005; accepted 28 July 2005

Available online 21 September 2005

Abstract

The thermal decomposition of adsorbed methanol on 2 wt.% Pd/silica, 2 wt.% Pd/gallia and pure gallia, was studied by temperature-programmed surface reaction (TPSR), between 323 and 723 K under He flow, using FT-IR spectroscopy. After methanol adsorption on Pd/silica at 323 K, the concentration of methoxy species on the silica decreased during the TPSR experiment, but some methoxy groups still remained on this support even at 723 K. Simultaneously, methanol decomposed over metallic palladium to yield, stepwise, HCO and CO with the consequent release of H₂ (g). On clean gallia, methanol is Lewis-bound adsorbed to the surface, as well as dissociatively adsorbed as methoxy (CH₃O), but the position of the infrared bands indicates a stronger interaction of these species on gallium oxide than on silica. Methoxy species on gallia are decomposed to (mono- and bi-dentate) formate groups (m- and b-HCOO, respectively) at $T > 473$ K. We suggest that CO and CO₂ are further produced by non-stoichiometric transformation of these formates, leading to the release of atomic hydrogen on the surface of the oxide, as detected by the Ga–H stretching infrared band, and surface anion vacancies. In the presence of Pd on the gallia surface, the dehydrogenation of CH₃O species proceeds faster than over the pure oxide, and we propose the following mechanism for methanol decomposition: (i) methanol reacts with OH groups on the gallia surface to produce water and methoxy species, (ii) the dehydrogenation of the latter carbonaceous group leads to H₂COO, first, and then to m- and b-HCOO, (iii) the hydrogen atoms released in the previous steps are transferred from gallia to the Pd surface where they recombine and desorb as H₂ (g).

© 2005 Elsevier B.V. All rights reserved.

Keywords: Methanol decomposition; Gallium oxide; Palladium catalyst; Hydrogen production

1. Introduction

In the past decade, significant R&D effort has been focused on reducing the emissions generated by internal combustion engines (ICEs). Since then, the use of hydrogen in proton-exchange membrane (PEM) fuel cells, for their use in mobile sources, has progressively gained importance [1]. Compared with conventional ICEs, lower emission of hazardous compounds and higher thermal efficiency have been mentioned as the main benefits derived from the utilization of fuel cells. However, both cost and safety issues involved in storage, handling and supply of hydrogen, make ‘on-board hydrogen generation’ the most convenient alternative [1]. To this end, several liquids fuels, such as alcohols and liquid hydrocarbons, have been considered for ‘on-board reforming’ technologies [1]. In particular, methanol is regarded as the most suitable

choice, because it has a high hydrogen-to-carbon ratio and, in comparison with alkane or higher alcohol reforming, methanol reforming shows lower selectivity to by-products, such as carbon monoxide and methane. Also, methanol has no C–C bonds, which reduces the risk of catalyst coking [2–6].

One of the most promising reforming processes for hydrogen production from methanol is steam reforming (SRM): CH₃OH + H₂O = 3H₂ + CO₂ [1,2,7]. However, methanol decomposition, which is a strongly endothermic reaction, frequently occurs alongside with the main reaction and it is seen, together with the reverse water gas shift reaction, as the responsible of the production of CO in the system [4,8–10]. As it is well known, CO concentration has to be reduced downstream, to avoid poisoning of the platinum electrode of the PEM fuel cell [1].

The use of Pd-based catalysts for SRM (among which palladium supported onto reducible oxide supports have shown the higher selectivity to carbon dioxide and activity to hydrogen) has been recently reported in the literature [3,11–

* Corresponding author. Tel.: +54 342 4559175; fax: +54 342 4550944.

E-mail address: aboni@intec.unl.edu.ar (A.L. Bonivardi).

13]. Iwasa et al. studied the SRM reaction on Pd supported over ZnO, In₂O₃, Ga₂O₃, SiO₂, MgO, ZrO₂ and CeO₂, at 493 K, using a water-to-methanol ratio equal to 1 [11]. They found that Ga₂O₃, In₂O₃ and ZnO gave the most active materials, as compared to Pd/SiO₂, with selectivity to CO₂ higher than 95% in all cases. Nevertheless, methyl formate was the main product when only methanol was fed to the reactor, at 473 K, on these supported Pd catalysts. Further work of Iwasa et al. using Pd-based materials confirmed that the selectivity and activity of the SRM is improved by the addition of Zn, Cd, In and Ga oxides to their Pd/CeO₂ base formulation [12].

In a previous work some of us proved that methanol could be successfully synthesized on Ga₂O₃-Pd/SiO₂ catalysts [14] from a mixture of CO₂ and H₂ (that is, the SRM reverse reaction). Later on, we presented a mechanism for the synthesis of methanol from carbon dioxide on Pd/gallia [15].

It seems but logical, then, that a better understanding of the selective catalytic production of hydrogen from the steam reforming of methanol can be achieved by jointly studying the interaction of methanol with the pure metal oxides and with Pd supported onto them.

In this regard, we report here the results of temperature-programmed surface reaction experiments, followed by in situ Fourier transform infrared spectroscopy (FT-IR), on the adsorption and decomposition of methanol on pure Ga₂O₃ and Pd/Ga₂O₃.

2. Experimental

2.1. Catalysts

Pd/SiO₂ (2 wt.% Pd) was obtained by ion exchange of Pd(II) acetate (Sigma, 99.97%) onto silica (Davison 59; BET surface area = 301 m²/g) at pH 11 in NH₄OH (aq). The exchanged material was washed at the same pH, and dried at 423 K. The resulting diammine palladium complex was then calcined in flowing air (200 cm³/min), by heating from 298 to 673 K (2 h) at 2 K/min to obtain dispersed PdO on the surface. The PdO/SiO₂ was reduced in a 5% (v/v) H₂/Ar mixture (200 cm³/min), heating from 298 to 723 K (2 h) at 2 K/min. Finally, the catalyst was passivated at 298 K by flowing O₂/Ar mixtures (200 cm³/min) with increasing O₂ content, from 0.1 to 5% (v/v). The Pd metal dispersion of the reduced catalyst, measured by CO dynamic-pulse-chemisorption, was equal to 58%.

α- and β-Ga₂O₃ were obtained from Ga(NO₃)₃·xH₂O (Strem, 99.99 wt.% Ga) as previously described [16]. The presence of single crystallographic phases was verified by XRD (Shimadzu model XD-D1 diffractometer; Cu Kα radiation). The specific surface area of the gallia polymorphs was measured by the BET isotherm (N₂, 77 K) in a Micromeritics Accusorb 2001E unit: 20 and 64 m²/g for α- and β-Ga₂O₃, respectively.

Pd/α,β-Ga₂O₃ (2 wt.% Pd) catalyst was prepared by incipient impregnation of a commercial α,β-Ga₂O₃ (Strem, 99.998% Ga) with Pd(II) acetate (Sigma, 99.97%) in acetone. The “wet” precursor was air dried at 343 K for 1 h to get Pd(AcO)₂/α,β-Ga₂O₃. This material was then calcined in flowing air (673 K, 2 h) to obtain dispersed PdO on the surface. The PdO/α,β-Ga₂O₃

was reduced (723 K, 2 h) and passivated (298 K), with the same protocol used with Pd/SiO₂. The BET surface area was 21 m²/g and the Pd metal dispersion was equal to 8%.

2.2. FT-IR experiments

In situ transmission infrared spectroscopy was performed using aliquots (30 mg/ea.) of Pd/α,β-Ga₂O₃, α- or β-Ga₂O₃, and 10 mg for Pd/SiO₂, which were pressed into self-supporting wafers (dia. = 13 mm) at 5 t/cm². These wafers were placed, in turn, into a Pyrex[®] IR cell, with water-cooled NaCl windows, which was attached to a conventional high-vacuum system (base pressure = 1.33 × 10⁻⁴ Pa), equipped with a manifold for gas flow. Before any experiment was done, and to remove the artificial bands in the 3000–2800 cm⁻¹ region that arise from oil contamination during wafer preparation, each sample was exposed to the following pre-treatment procedure: first, O₂ was admitted into the cell (100 cm³/min) and the temperature was raised from 298 to 723 K at 5 K/min and immediately lowered to 323 K under He flow. Next, the cell was heated to 723 K at 5 K/min under H₂ (100 cm³/min). After 30 min at this last temperature the flow was switched to He (60 cm³/min) and kept for another 20 min at 723 K. Finally, the temperature was gradually decreased under He flow, to allow reference IR spectra of the “clean wafer” to be taken.

Methanol (Carlo Erba RPE, 99.9%) was purified by a series of freeze–thaw cycles under vacuum to remove dissolved gases and stored (298 K) in a glass bulb attached to the manifold. Afterwards, methanol vapor was allowed into a small section of the manifold (which featured a sampling loop), and then swept from the loop by flowing He (60 cm³/min) and admitted into the IR cell, at 323 or 373 K (see below). After methanol adsorption onto the catalyst wafer, the cell was purged for 30 min by flowing He at 60 cm³/min. Lastly, the temperature was decreased to 323 K. IR spectra were taken every 5 min along the process.

The temperature-programmed surface reaction (TPSR) experiments were performed over each methanol pre-treated sample, by heating the IR cell from 323 to 723 K at 10 K/min under flowing He (60 cm³/min). A transmission infrared spectrum was recorded every 25 K.

A Shimadzu 8210 FT-IR spectrometer with a DLATGS detector (4 cm⁻¹ resolution, 100 scans) was used to acquire the spectra. Further processing of the data was carried out with the Microcal Origin[®] 4.1 software.

H₂ (AGA UHP grade 99.999%) and He (AGA UHP 99.999%) were further purified prior to use using molecular sieve (3 Å Fisher) and MnO/Al₂O₃ traps, to remove water and oxygen impurities. O₂ (AGA Research grade 99.996%) was passed through a molecular sieve (3 Å Fisher) and an Ascarite[®] trap, to remove water and CO₂.

3. Results and discussion

3.1. Decomposition of methanol on Pd/SiO₂

Methanol decomposes extensively on silica-supported Pd at 373 K. Therefore the adsorption of CH₃OH (g) on the clean Pd/

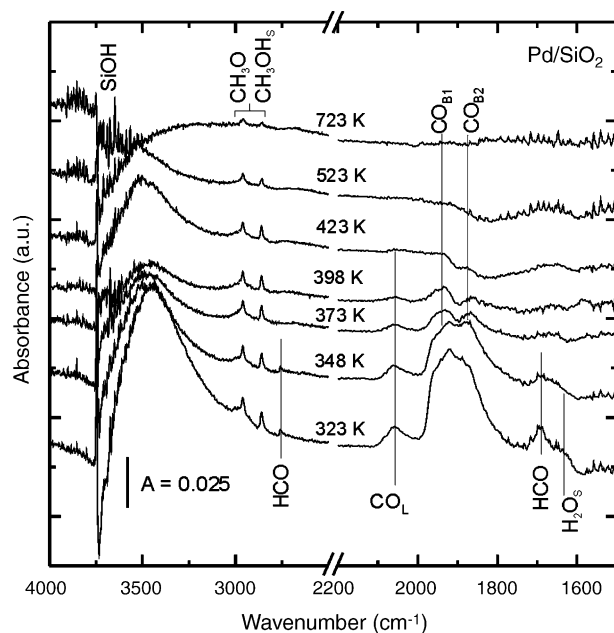


Fig. 1. IR spectra during the temperature-programmed surface reaction (TPSR) of adsorbed methanol on Pd/SiO₂.

SiO₂ catalyst was performed at 323 K. After purging the cell in flowing He (30 min), various species were detected on the catalyst surface (Fig. 1). Several bands appeared in the CH stretching region (Table 1), which are identical to the ones obtained after exposing pure SiO₂ to methanol [17]. The most intense signals, at 2960 and 2860 cm⁻¹, are frequently assigned to the symmetric and asymmetric CH stretching of adsorbed methoxy, $\nu_{\text{as}}(\text{CH}_3)$ and $\nu_{\text{s}}(\text{CH}_3)$, respectively. However, a more detailed IR analysis based on the adsorption of methanol on activated Al₂O₃ [18], quantum mechanic calculations of methoxy species on Cu(100) [19] and the use of model molecules such as methanol, methyl esters and dimethyl ether [20], allowed us to conclude that a more realistic assignment is the following. The high frequency bands correspond to two strongly adsorbed species, methanol (CH₃OH_s) and methoxy (CH₃O) on the support surface. The $\nu_{\text{as}}(\text{CH}_3)$ mode gives a weaker band at higher frequency than the $\nu_{\text{s}}(\text{CH}_3)$ mode. Thus, the 2997 cm⁻¹ signal is assigned to the asymmetric stretching of CH of both surface species, while their $\nu_{\text{s}}(\text{CH}_3)$ mode can be

resolved into two bands, at 2961 (CH₃OH_s) and 2952 (CH₃O) cm⁻¹. The weak, overlapped band at lower frequency, 2925 cm⁻¹, is assigned to the $2\delta_{\text{as}}(\text{CH}_3)$ overtone of methanol and methoxy species, and the band at 2859 cm⁻¹ is the result of the overlapping of the overtones of the CH symmetric deformation, $2\delta_{\text{s}}(\text{CH}_3)$. Unfortunately, the least intense bands – proper of the $\delta_{\text{as}}(\text{CH}_3)$, $\delta_{\text{s}}(\text{CH}_3)$ and in plane $\delta(\text{OH})$ modes – remained undetected under our experimental conditions.

The broad band centered around 3500–3300 cm⁻¹ decreased in intensity during the IR cell purge with He flow. This band corresponds, in part, to the $\nu(\text{OH})$ mode of adsorbed methanol on the silica surface. The strong downshift of the signal with respect to gaseous methanol (3645 cm⁻¹), together with the appearance of a negative band at 3730 cm⁻¹ due to the loss of isolated terminal silanol groups (SiOH), suggest strong hydrogen bonding between the surface OH groups and methanol. Concurrently with the methanol adsorption, a band at 1629 cm⁻¹ due to adsorbed water [$\delta(\text{OH})$ mode] showed up over Pd/SiO₂. This can be readily interpreted as some amount of water produced between surface OH groups and H coming from methoxy formation.

Additionally, other features arose in the 2200–1700 cm⁻¹ region during the methanol adsorption on Pd/SiO₂ (see Fig. 1). The integrated intensity of these signals increased during the exposure to gaseous methanol and then remained constant throughout the He purge at 323 K. These bands, at 2060, 1930 (broad and overlapped), and 1875 cm⁻¹ are due to CH₃OH decomposition on the palladium surface and correspond to chemisorbed carbon monoxide (CO_s) on Pd [21]. The band above 2000 cm⁻¹ is attributed to terminal, mono-coordinated or linearly bonded CO (CO_L), while the broad, convoluted bands below 2000 cm⁻¹ are assigned to multi-coordinated, bridging CO (CO_B). The latter have been further classified from single-crystal studies as CO_{B1}, corresponding to dicoordinated bridging CO on structurally open crystal planes such as (1 0 0) or (2 1 0), close to 1970 cm⁻¹, and CO_{B2}, corresponding to dicoordinated CO on Pd(1 1 1), around 1900 cm⁻¹ [21].

Two other bands can be discerned after the methanol adsorption process, at 2759 and 1708 cm⁻¹, and are both assigned to the $\nu(\text{CH})$ and $\nu(\text{CO})$ modes of formyl groups (HCO) chemisorbed onto the palladium crystallites [22].

As the temperature of the IR cell was increased from 323 to 723 K, the bands originated by methanol and water adsorbed on

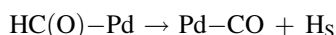
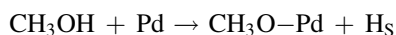
Table 1
Infrared bands for methanol and methoxy species on Pd/SiO₂, Ga₂O₃ and Pd/Ga₂O₃

Vibrational mode	Pd/SiO ₂		β-Ga ₂ O ₃ or Pd/α,β-Ga ₂ O ₃		α-Ga ₂ O ₃	
	CH ₃ OH _s (cm ⁻¹)	CH ₃ O (cm ⁻¹)	CH ₃ OH _s (cm ⁻¹)	CH ₃ O (cm ⁻¹)	CD ₃ OH _s (cm ⁻¹)	CD ₃ O (cm ⁻¹)
$\nu_{\text{as}}(\text{CH}_3 \text{ or } \text{CD}_3)$	2997	2997	2990	2990	2257	2257
$\nu_{\text{s}}(\text{CH}_3 \text{ or } \text{CD}_3)$	2961	2952	2958	2940	2071	2060
$2\delta_{\text{as}}(\text{CH}_3 \text{ or } \text{CD}_3)$	2925	2925	2907	2907	2135	2135
$2\delta_{\text{s}}(\text{CH}_3 \text{ or } \text{CD}_3)$	2859	2859	2836	2836	2222	2197
$\delta_{\text{as}}(\text{CH}_3 \text{ or } \text{CD}_3)$	–	–	1510	1510	1032	1032
$\delta_{\text{s}}(\text{CH}_3 \text{ or } \text{CD}_3)$	–	–	1468	1468	1110	1110
$\rho(\text{CH}_3 \text{ or } \text{CD}_3)$	–	–	1183	1126	–	–
$\nu(\text{CO})$	–	–	1030	1070	960	1027

Pd/SiO₂ progressively faded out, together with the recovery of the base line at 3730 cm⁻¹, that is, of the isolated silanol (SiOH) groups.

Fig. 2 shows the thermal evolution of the intensity of the most relevant IR bands of the surface species. The concentration of stable methoxy species steadily decreased with heating, but they still remained on the surface of the silica even at 723 K [17]. Concurrently, the concentrations of HCO and CO_S also decreased on the palladium surface, but neither CO_L nor CO_B were present from 448 K onward. The intensity of the 1708 cm⁻¹ band almost mimicked that of CO's, vanishing from 423 K.

Several authors agree that methanol decomposition, CH₃OH → CO + 2H₂, proceeds fast on the palladium surface, even at sub-ambient temperature [17,22]. Moreover, IR signals attributed to CH₃OH–Pd and CH₃O–Pd were observed by exposing Pd/SiO₂ to methanol even at 213 K [17]. Further, formyl groups and adsorbed formaldehyde have been postulated as surface intermediates in the catalytic decomposition of methanol on Pd and Cu catalysts [17,22,23]. Thus, the mechanism of methanol decomposition over Pd/SiO₂ is envisioned as follows:



That is, chemisorbed methoxy species lose surface hydrogen (H_S) stepwise to give formyl and CO_S entities; and H_S atoms recombine to desorb as H₂.

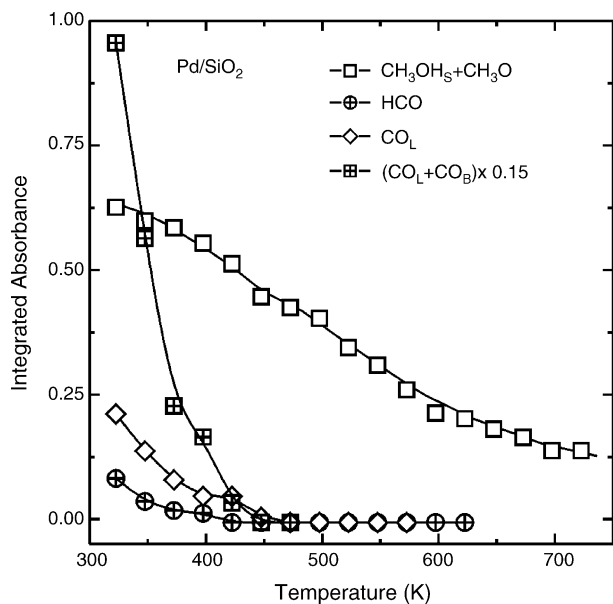


Fig. 2. Evolution of the integrated intensity of the IR bands of the surface species during the TPSR of adsorbed methanol on Pd/SiO₂: 3000–2800 cm⁻¹ (CH₃OH_S + CH₃O), 1708 cm⁻¹ (HCO), 2060 cm⁻¹ (CO_L) and 2000–1800 cm⁻¹ (CO_{B1} + CO_{B2}).

3.2. Decomposition of methanol on Ga₂O₃

Fig. 3 displays the infrared spectra obtained after the adsorption/decomposition of methanol on the surface of β-Ga₂O₃ at 373 K.

The IR spectrum at 323 K indicates that methanol exposure at 373 K produces both associatively adsorbed, intact methanol, Lewis-bound to the surface (CH₃OH_S), as well as dissociatively adsorbed methoxy (CH₃O) [18,24–26]. The frequencies of the IR bands, which are typical of these species, are shown in Table 1. The CH stretching and bending overtone modes of each species were also present in the Pd/SiO₂ spectrum at 323 K, but at higher frequencies, which indicates a stronger interaction of methanol and methoxy on gallium oxide than on silica.

In the high frequency region (>3000 cm⁻¹) a broad band developed between 3500 and 3300 cm⁻¹, mainly due to the ν(OH) mode of molecularly adsorbed methanol. The negative band at approximately 3650 cm⁻¹, alongside with the methanol adsorption, has to be ascribed to the depletion of different types of surface hydroxyl groups of the gallia [27]. The δ(OH) mode at 1630 cm⁻¹, which is usual in the presence of molecularly adsorbed water on different oxides, was not observed on the β-Ga₂O₃, probably due to the high temperature of methanol adsorption and further He purging. Actually, in an extra experiment using mass spectrometry we were able to detect gaseous water upon adsorbing methanol on gallia under identical experimental conditions to the ones used in this study.

The transparency of gallia in the low frequency region (<1550 cm⁻¹), as opposed to silica, allowed us to detect the CH₃ bending and rocking vibrations (1510, 1468, 1183 and 1126 cm⁻¹), and the CO stretching mode (1070 and 1030 cm⁻¹) of both methoxy and methanol groups. A negative band below 900 cm⁻¹ was observed (Fig. 3), and it is attributed

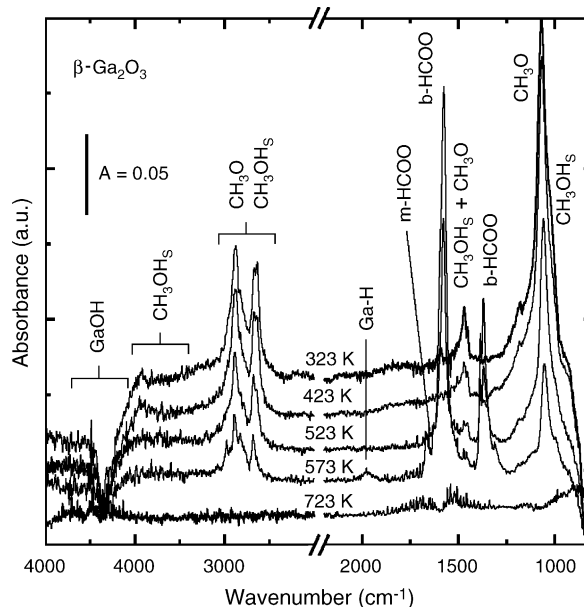


Fig. 3. IR spectra during the TPSR of adsorbed CH₃OH on β-Ga₂O₃.

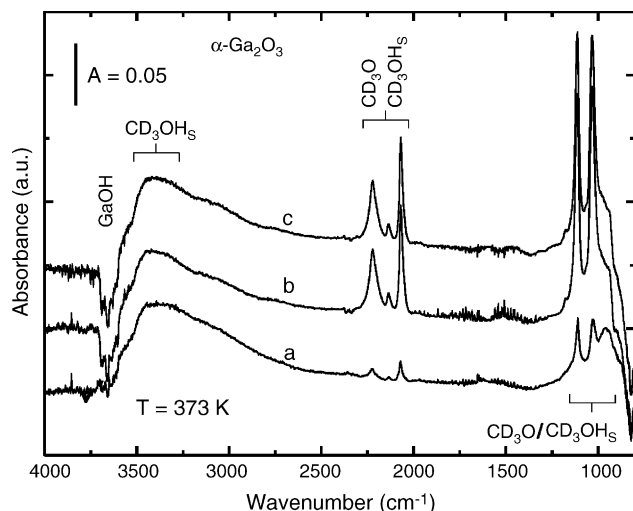


Fig. 4. IR spectra of CD_3OH adsorption on $\alpha\text{-Ga}_2\text{O}_3$ at 373 K after 0.5 min (a) and 3 min (b) of exposure, and after purging for 30 min by flowing He at $60\text{ cm}^3/\text{min}$ (c).

to the perturbation of the surface Ga–O–Ga mode, like that of the Al–O–Al mode in $\delta\text{-Al}_2\text{O}_3$ [18].

In addition, we run a CD_3OH adsorption experiment on $\alpha\text{-Ga}_2\text{O}_3$ at 373 K. After exposing the gallium oxide to methanol- d_3 during 0.5 min typical infrared bands of CD_3OH_s and CD_3O species were detected (Fig. 4 and Table 1). The experimental values for the ratio between the stretching frequencies of C–H and C–D bonds was 1.37 ± 0.05 , which is fairly close to the expected one for the $\nu(\text{C–H})$ versus the $\nu(\text{C–D})$ symmetric or asymmetric modes, i.e., 1.36. The C–D deformation modes and their overtones were further assigned according to literature data based on the adsorption of CD_3OH on activated alumina

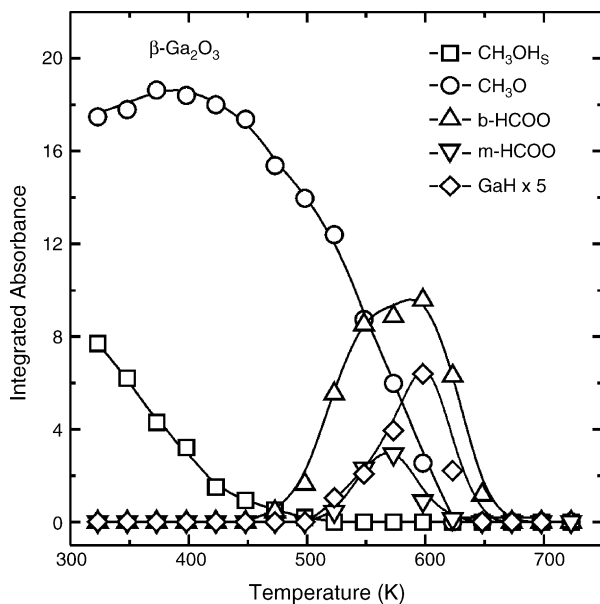
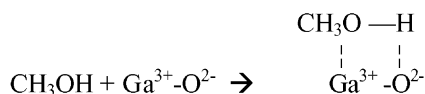


Fig. 5. Evolution of the integrated intensity of the IR bands of the surface species during the TPSR of adsorbed methanol on $\beta\text{-Ga}_2\text{O}_3$: 1030 cm^{-1} (CH_3OH_s), 1070 cm^{-1} (CH_3O), 1580 cm^{-1} (b-HCOO), 1640 cm^{-1} (m-HCOO) and 1990 cm^{-1} (Ga–H).

and CD_3OH monomer in CCl_4 solution [18]. Fig. 4 also shows that CD_3OH adsorption on gallia at 373 K consumed surface OH groups (a negative band at approximately 3650 cm^{-1} showed up after 3 min of exposure to deuterated methanol), which are partially transformed to gaseous H_2O , as revealed by the several bands around 1600 cm^{-1} . Together with water release, the enrichment of surface methoxy species occurred: the intensity of the C–D stretching and bending modes notoriously increased, while the broad band developed between 3500 and 3300 cm^{-1} , due to the $\nu(\text{OH})$ mode of molecularly adsorbed methanol- d_3 , remained constant. It is important to notice that we did not observe any isotopic scrambling between CD_3OH and the gallia surface at 373 K.

Next, after the adsorption of methanol- d_3 , the cell was purged under flowing He at 373 K, as described in Section 2. The resulting infrared spectrum (Fig. 4c) shows that most of the methoxy species, as well as adsorbed methanol, still remained on the surface of the α -gallium oxide, as was the case on the beta phase.

Summarizing, the adsorption of methanol on gallia at 373 K can be written as:



The TPSR experiment $\beta\text{-Ga}_2\text{O}_3$ showed the decrease of CH_3OH_s species at increasing temperature, to vanish at 500 K (Figs. 3 and 5). The concentration of methoxy groups grew slightly at first ($T < 423\text{ K}$), but promptly diminished, and finally disappeared at 623 K.

From 473 K onwards, that is, from the sharp consumption of methoxy group, several peaks emerged in the $1650\text{--}1300\text{ cm}^{-1}$ region, which were assigned to monodentate and bidentate formate species on gallia (m- and b-HCOO, respectively, in Table 2). The CH stretching vibration of b-HCOO species was located at 2898 cm^{-1} , and the combination band [$\nu_{\text{comb}} = -\nu_{\text{as}}(\text{CO}_2) + \delta(\text{CH})$] at 2991 cm^{-1} (see also Fig. 3). The unambiguous assignment of the full set of bands was reported in a previous work using isotopic exchange experiments [15].

The surface concentration of both formate groups reached a maximum at 573 K, and from 673 K these species became undetectable.

The thermal evolution of the formate species was followed by the appearance of Ga–H on the surface of gallia, as revealed by the GaH stretching band at approximately 1990 cm^{-1}

Table 2
Infrared bands for bidentate and monodentate formate species on Ga_2O_3

Vibrational mode	m-HCOO (cm^{-1})	b-HCOO (cm^{-1})
$\nu_{\text{as}}(\text{COO})$	1640	1580
$\nu_{\text{s}}(\text{COO})$	1298	1372
$\delta(\text{CH})$	1350	1386
$\nu(\text{CH})$	–	2898
ν_{comb}^a	–	2991

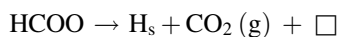
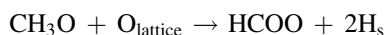
^a $\nu_{\text{comb}} = \nu_{\text{as}}(\text{CO}_2) + \delta(\text{CH})$.

(Fig. 3) [16,28]. However, no signals proper to formyl or formaldehyde species were observed over the bare gallium oxide at any temperature.

Another interesting feature of the IR spectra during the decomposition of methanol on gallium oxide was the progressive recovery of the Ga–OH surface groups [that is, of the $\nu(\text{OH})$ band] along the entire temperature ramp. Up to 523 K, the partial desorption of methanol could be a suitable explanation, but other surface reaction has to take place to account for the development of these OH groups at higher temperatures. For example, formate species can be synthesized over the gallia surface either by reaction between Ga–H species and adsorbed CO_2 (as carbonates) [15] or by reactive chemisorption of CO gas into Ga–OH sites [29]. Hence, the reverse reactions can also occur over the gallia surface. Once again, the abovementioned mass spectrometry experiment confirmed the release of CO and CO_2 to the gas phase during the decomposition of the formate groups. At >600 K, the Ga–H and Ga–OH species recombine, releasing H_2 (g), and leaving Ga–O–Ga surface groups [16].

The absence of surface carbonate species as a product of the formate decomposition was expected, because carbonates are weak intermediates that can be formed on the surface of gallia only under the continuous presence of CO_2 in the gas phase [15,29].

According to these combined observations, the decomposition of methoxy species over the gallia surface proceeds as follows:



where \square stands for an oxygen vacancy.

We believe that the most likely surface intermediate for the first reaction, that is: methoxy to formate, is the methylene-bisoxo (or dioxymethylene) species (hereafter, H_2COO). This last surface group has been experimentally identified and postulated as an intermediate for the oxidation or decomposition of methanol and formaldehyde over the surface of several oxides or mixed oxides. In particular, the oxidation of methanol on vanadium–titanium oxide catalysts has been rationalized as a stepwise process that begins with the condensation of methanol on surface VOH groups, followed by the oxidation of methoxy groups to give adsorbed formaldehyde species, which are further attacked by a nucleophilic site of the surface of the catalyst (surface lattice oxygen) producing methylene-bisoxo species. The last group is then oxidized to formates, which can react with methanol to give methylformate, or with water to produce formic acid, or can decompose to give carbon oxides [30–32].

The same sequence of elementary steps from methoxy to the dioxymethylene intermediate was also proposed for the decomposition of methanol over the $\text{ZrO}_2(110)$ surface [33]. Specifically, Dilara and Vohs followed by HREELS the

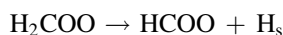
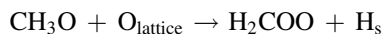
vibration frequencies of dioxymethylene on the $\text{ZrO}_2(110)$ plane, a surface with oxygen atoms in the first layer available to produce the nucleophilic attack on methoxy groups [33]. By contrast, they did not distinguish the dioxymethylene species on the $\text{ZrO}_2(100)$ surface, i.e., where oxygen atoms are present in the second surface layer [33]. Furthermore, the methoxy groups adsorbed on reduced ceria–zirconia mixed oxides could produce dioxymethylene or polyoxymethylene species as O_2 was added in doses to the sample at room temperature [34]. More recently, Mensch et al. [35] suggested that the reaction of methanol on the nearly stoichiometric $\alpha\text{-Cr}_2\text{O}_3(1012)$ surface (which gave a spectrum of products: CH_4 , CH_2O , CO and CO_2), occurs through a reaction pathway involving surface dioxymethylene species as the primary bidentate intermediate.

The formation of methylene-bisoxo species, other than over surface metal oxides, has also been identified in organometallic compounds. Tardif et al. [36] succeeded at hydrogenating CO_2 into methylene diolate (or dioxymethylene) by CO_2 insertion in a tetranuclear tetrahydrido yttrium complex, at 273 K. Likewise, to understand the synthesis of methanol from CO_2 hydrogenation, Schlörer and Berger [37] studied the reaction of CO_2 with $\text{Cp}_2\text{Zr}(\text{H})\text{Cl}$ by in situ variable-temperature ^{13}C NMR, reporting a peak at $\delta = 101.2$ attributed to the CH_2 carbon signal of the dioxymethylene intermediate, which promptly disappeared, at 300 K. Therefore, as a general rule the methylene-bisoxo species seems to be very unstable, even a room temperature, which can explain why it is only clearly detected after specifically designed experiments, for example via the direct adsorption of formaldehyde on various metal oxides, such as TiO_2 , ZrO_2 and ThO_2 at 240–270 K [38].

Thus, and because the surface methylene-bisoxo species was not explicitly identified on Ga_2O_3 in our TPSR experiments, we can justifiably assume that under our experimental conditions this species is unstable on the gallium oxide, and that it rapidly transforms to either m- or b-formate groups [15].

The methanol decomposition process involves a nucleophilic attack by surface lattice oxygen atoms. This fact can be understood if we consider that Ga_2O_3 is a reducible oxide that can be partially reduced to Ga_xO [28,39]. Hence, labile O atoms from the oxide lattice are able to attack the carbon atom of the methoxy species leading to dioxymethylene groups, which further decompose to formate, and H on top of reduced surface gallium ion, as detected by the $\nu(\text{Ga–H})$ signal (Fig. 5).

Then, we suggest that over oxide catalysts like Ga_2O_3 , which has proved to be active for the production of methylformate from methanol [11], the main elementary steps of hydrogen abstraction of the methoxy group to formate are the following:



in agreement with Fisher and Bell [23], who proposed similar elementary steps for the decomposition of methanol over a $\text{Cu–ZrO}_2/\text{SiO}_2$ catalyst.

Finally, it is worth noticing that we have shown in a previous work that the amount and coordination (octahedral or tetrahedral) of Ga^{3+} surface cations of the different gallia

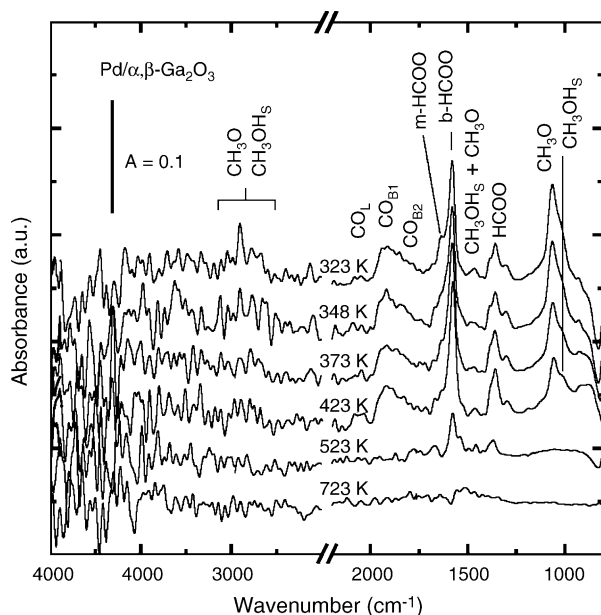


Fig. 6. IR spectra during the TPSR of adsorbed methanol on Pd/ α,β -Ga₂O₃.

polymorphs can be determined by H₂ adsorption. On the surface of the β -gallia half of these Ga³⁺ cations are in octahedral coordination, while only this type of coordinated cations prevails on α -gallia [16]. However, we did not find any different IR signal on the alpha phase other than those observed over the beta phase, after methanol adsorption/decomposition. Consequently, we do not expect a different chemical behavior for the α,β -Ga₂O₃ material used in this work to obtain the Pd supported gallia catalyst.

3.3. Decomposition of methanol on Pd/ α,β -Ga₂O₃

The adsorption of methanol on Pd/ α,β -Ga₂O₃ at 373 K led not only to the formation of adsorbed methanol and dissociatively adsorbed methoxy species but also to the earlier decomposition of such groups, as compared to the pure gallia, to yield both *m*- and *b*-formate species on gallia and chemisorbed CO on Pd. The main IR bands of these species are shown in Fig. 6.

During the TPSR ramp in flowing He, the surface concentration of CH₃OH_s and CH₃O species continually decreased, until they disappeared over 473 K (Figs. 6 and 7). Concurrently, the amount of *m*-formate came up to a maximum at 350 K and *b*-formate reached their highest coverage at ca. 400 K. The interconversion between *m*- and *b*-formate species was already underscored in a previous work of us [15], as well as the higher thermal stability of the bidentate group, which remains over the gallia surface up to 600 K. So, as the *b*-formate band begins to lose intensity at about 50 K higher temperature than that of *m*-formate, this might well be ascribed, again, to the transformation of *m*- into *b*-HCOO prior to further decomposition.

Like on Pd/SiO₂, methanol partially decomposed on the disperse metal in the Pd/ α,β -Ga₂O₃ catalyst, leaving chemisorbed CO [$\nu(\text{CO}_L) = 2060 \text{ cm}^{-1}$, $\nu(\text{CO}_{B1}) = 1913 \text{ cm}^{-1}$ and

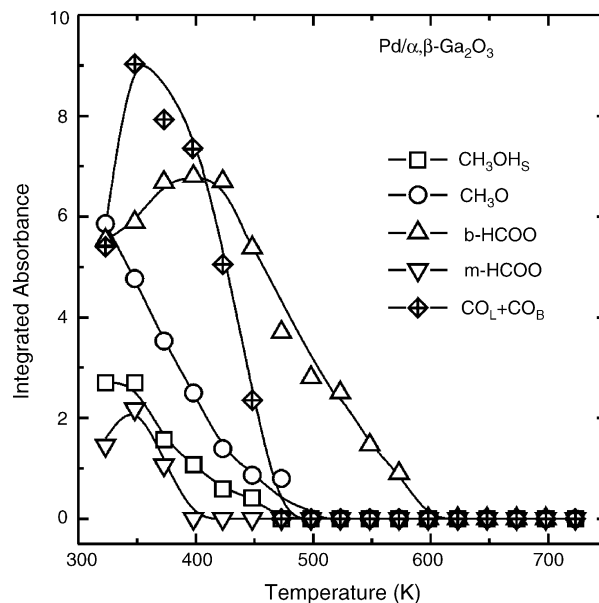


Fig. 7. Evolution of the integrated intensity of the IR bands of the surface species during the TPSR of adsorbed methanol on Pd/ α,β -Ga₂O₃: 1030 cm⁻¹ (CH₃OH_s), 1070 cm⁻¹ (CH₃O), 1580 cm⁻¹ (*b*-HCOO), 1640 cm⁻¹ (*m*-HCOO) and 2100–1800 cm⁻¹ (CO_L + CO_{B1} + CO_{B2}).

$\nu(\text{CO}_{B2}) = 1850 \text{ cm}^{-1}$]. The bands corresponding to CO_S evolved up to ca. 375 K and then decreased during the temperature ramp (Fig. 7). CO_L and CO_{B1} were the first species to disappear, at 400 K, while CO_{B2} groups remained up to ca. 500 K. Unfortunately, we could not detect any vibration mode of formyl species on this catalyst, most likely due to the low metal dispersion in the Pd/ α,β -Ga₂O₃ (8%) as compared to the Pd/SiO₂ (58%).

Our investigation of methanol synthesis from CO₂/H₂ has shown that HCOO and CH₃O are formed at lower temperatures, and at higher rates, on Pd/ β -Ga₂O₃ than on clean β -Ga₂O₃ [15]. We suggested in that work that the hydrogen required for these hydrogenation reactions to take place is supplied by H₂ spillover from Pd to the oxygenated carbonaceous intermediates located on gallia.

During the decomposition of adsorbed methanol on gallia and Pd/gallia, the conversion of CH₃O to HCOO requires a sink for atomic hydrogen, and labile oxygen atoms, to proceed (from the gallia lattice, for example). Certainly, we showed that Ga–H species are formed on pure gallium oxide. Nevertheless, in the presence of metallic palladium on the gallia surface, the dehydrogenation of methoxy groups progresses faster than over the clean oxide. Then, it seems reasonable to suggest, once more, that H₂ atoms are transferred from Ga₂O₃ to Pd by reverse spillover, where they finally recombine and desorb as H₂ (g). Lastly, we emphasize again that the oxygen atoms able to transform methoxy species to formate groups are provided by the support; furthermore the reducibility of gallium oxide is enhanced by the presence of noble metals, such as Pd [14,28] or Pt [40]. Thus, in like manner as on clean gallia, surface oxygen atoms of the support react with methoxy groups to yield dioxymethylene species which further transform to formate groups on the Pd/gallia catalyst.

In summary, we suggest the following rational mechanism for methanol decomposition on Pd/ α,β -Ga₂O₃: The methanol molecules interact with OH groups on the gallia surface to give methoxy species. The stepwise dehydrogenation of the latter leads to methylene-bisoxo, first, and then to m- and b-HCOO on gallia. The hydrogen atoms released from the carbonaceous species are transferred from the gallium oxide surface to the Pd crystallites. The products, CO, CO₂, H₂ and H₂O, are the result of the described bifunctional pathway for the methanol decomposition on the Pd–Ga₂O₃ system. Additionally, but in a much lower extension, some methanol is also decomposed on metallic palladium to yield CO and H₂.

It seems clear, then, that in the SRM reaction on this system, water provides the oxygen atoms needed to replenish the oxygen vacancies on the surface of the gallium oxide. Thus, the high selectivity to CO₂ reported by Iwasa et al. [11] during the SRM on Pd/gallia, as compared to Pd/SiO₂, can be justly explained. However, if only methanol is (continuously) fed into the reactor at 473 K, that is, when only b-HCOO and CH₃O predominate over the surface of Pd/gallia catalysts (Fig. 7), the main expected product is methylformate [11].

Acknowledgements

This work was supported by the Consejo Nacional de Investigaciones Científicas y Técnicas (CONICET) and the Agencia Nacional para la Promoción de la Ciencia y la Tecnología (ANPCyT) of Argentina.

References

- [1] L. Carrette, K.A. Friedrich, U. Stimming, *Fuel Cells* 1 (2001) 5.
- [2] J.R. Rostrup-Nielsen, *Phys. Chem. Chem. Phys.* 3 (2001) 283.
- [3] J. Agrell, K. Hasselbo, K. Jansson, S.G. Järas, M. Boutonnet, *Appl. Catal. A* 211 (2001) 239.
- [4] B. Lindström, L.J. Petterson, *J. Power Sources* 118 (2003) 71.
- [5] J. Agrell, H. Birgersson, M. Boutonnet, I. Melián-Cabrera, R.N. Navarro, J.L. García Fierro, *J. Catal.* 219 (2003) 389.
- [6] P.H. Matter, D.J. Braden, U.S. Ozkan, *J. Catal.* 223 (2004) 340.
- [7] P.J. de Wild, M.J.F.M. Verhaak, *Catal. Today* 60 (2003) 3.
- [8] M. Turco, G. Bagnasco, U. Costantino, F. Marmottini, T. Montanari, G. Ramis, G. Busca, *J. Catal.* 228 (2004) 56.
- [9] J. Agrell, G. Germani, S.G. Järas, M. Boutonnet, *Appl. Catal. A* 242 (2003) 233.
- [10] F. Bocuzzi, A. Chiorino, M. Manzoli, *J. Power Sources* 118 (2003) 304.
- [11] N. Iwasa, T. Mayanagi, N. Ogawa, K. Sakata, N. Takezawa, *Catal. Lett.* 54 (1998) 119.
- [12] N. Iwasa, T. Mayanagi, W. Nomura, M. Arai, N. Takezawa, *Appl. Catal. A* 248 (2003) 153.
- [13] S. Liu, K. Takahashi, M. Ayabe, *Catal. Today* 87 (2003) 247.
- [14] A.L. Bonivardi, D.L. Chiavassa, C.A. Querini, M.A. Baltanás, *Stud. Surf. Sci. Catal.* 130D (2000) 3747.
- [15] S.E. Collins, M.A. Baltanás, A.L. Bonivardi, *J. Catal.* 226 (2004) 410.
- [16] S.E. Collins, M.A. Baltanás, A.L. Bonivardi, *Langmuir* 21 (2005) 962.
- [17] G.C. Cabilla, A.L. Bonivardi, M.A. Baltanás, *J. Catal.* 201 (2001) 213.
- [18] G. Busca, P.F. Rossi, V. Lorenzelli, M. Benaissa, J. Travert, J.C. Lavalley, *J. Phys. Chem.* 89 (1985) 5433.
- [19] M.P. Andersson, P. Uvdal, A.D. MacKerell Jr., *J. Phys. Chem. B* 106 (2002) 5200.
- [20] J. Derouault, J. Le Calve, M.T. Forel, *Spectrochim. Acta* 28A (1972) 359.
- [21] G.C. Cabilla, A.L. Bonivardi, M.A. Baltanás, *Catal. Lett.* 55 (1998) 147 (and references therein).
- [22] J. Raskó, J. Bontovics, F. Solymosi, *J. Catal.* 146 (1994) 22.
- [23] I.A. Fisher, A.T. Bell, *J. Catal.* 184 (1999) 357.
- [24] L.J. Burcham, M. Badlani, I.E. Wachs, *J. Catal.* 203 (2001) 104.
- [25] J.C. Lavalley, *Catal. Today* 27 (1996) 377.
- [26] G. Busca, *Catal. Today* 27 (1996) 457.
- [27] M. Rodríguez Delgado, C. Otero Areán, *Mater. Lett.* 57 (2003) 2292.
- [28] S.E. Collins, M.A. Baltanás, A.L. Bonivardi, *J. Catal.* 211 (2002) 252.
- [29] S.E. Collins, M.A. Baltanás, A.L. Bonivardi, unpublished results.
- [30] G. Busca, A.S. Elmi, P. Forzatti, *J. Phys. Chem.* 91 (1987) 5263.
- [31] F.S. Feil, J.G. van Ommen, J.R.H. Ross, *Langmuir* 3 (1987) 668.
- [32] A.S. Elmi, E. Tronconi, C. Cristiani, J.P. Gomez Matin, P. Forzatti, G. Busca, *Ind. Eng. Chem. Res.* 28 (1989) 387.
- [33] P.A. Dilara, J.M. Vohs, *Surf. Sci.* 321 (1994) 8.
- [34] C. Binet, M. Daturi, *Catal. Today* 70 (2001) 155.
- [35] M.W. Mensch, C.M. Byrd, D.F. Cox, *Catal. Today* 85 (2003) 279.
- [36] O. Tardif, D. Hashizume, Z. Hou, *J. Am. Chem. Soc.* 126 (2004) 8080.
- [37] N.E. Shlörer, S. Berger, *Organometallics* 20 (2001) 1703.
- [38] G. Busca, J. Lamotte, J.-C. Lavalley, V. Lorenzelli, *J. Am. Chem. Soc.* 109 (1987) 5197.
- [39] B.S. Kwak, W.M.H. Sachtler, *J. Catal.* 145 (1994) 456.
- [40] E.S. Shpiro, D.P. Shevchenko, M.S. Kharson, A.A. Dergachev, Kh.M. Minachev, *Zeolites* 12 (1992) 670.